COMPUTATIONAL SIMULATION OF MASS TRANSFER AND CHEMICAL REACTIONS AT COMPONENT SURFACES IN FLUIDISED BED HEAT TREATMENT FURNACES

Weimin GAO[1,2], Lingxue KONG[2], Daniel M. FABIJANIC[1] and Peter D. HODGSON[1]

[1] Deakin University, Geelong, Victoria 3217, AUSTRALIA

[2] University of South Australia, Mawson Lakes, South of Australia 5095, AUSTRALIA

ABSTRACT

The diffusion of gaseous species (CO, CO_2, H_2O, CH_4, H_2, O_2) and their chemical reactions have been computationally simulated to model carbon transfer at an immersed steel surface in a carburising fluidised bed of 0.1 mm alumina particles. The simulations of the gaseous molecule diffusion and the chemical reactions both in the bed and at the atmosphere/steel interface were implemented with FLUENT, while the particles were treated as a pseudo-continuous fluid phase and modelled with Eulerian multiphase flow model. The interactions between the gases and the solid particles, including the heat and kinetic energies and mass exchange, were included in the model.

INTRODUCTION

The mass transfer at the surface of steel components immersed in a fluidised bed heat treatment furnace is a complex physical and chemical process, which generally depends on hydrodynamics, species diffusion and chemical reactions (Gao, Long, Kong and Hodgson, 2004). In the chemical heat treatment fluidised bed, a bed of small solid particles (e.g. alumina) are transformed into a liquid-like state, supported by a carburising or nitrocarburising gas flow fed up through the bed. The fluidising gas is normally composed of two or more different gases. For example, a mixture of natural-gas and air react in the bed to create a carburising atmosphere. The process of mass transfer of the diffusion elements from the gas phase to the steel includes several steps (Collin, 1976):

(i)   chemical reactions in the gas phase,
(ii) diffusion in the boundary layer of the reacting gases towards the component surface and the reactants in the opposite direction,
(iii) reactions at the steel surface and,
(iv) diffusion of the elements into the steel.

The hydrodynamics of gas fluidised beds has been computationally studied with various methods, such as finite element method (van Wachem, Schouten, van den Bleek, Krishna and Sinclair, 2001a, Zheng, Wan, Qian, Wei and Jin, 2001), finite volume method and discrete element method (Tsuji, Kawaguchi and Tanaka, 1993, Rhodes, Wang, Nguyen, Stewart and Liffman, 2001a), however, most of these models have only concerned the motion of particles (Tsuji, et al., 1993, van Wachem, et al., 2001a, Gao, Hodgson and Kong, 2005), seldom considering the species diffusion and chemical reactions (Gao, et al., 2004). In modelling the element diffusion, a simple boundary was normally used for the part surface. The simulation of species diffusion in a steel surface and the calculation of chemical reaction rate at the furnace-part interface are isolated from the hydrodynamic simulation. By this means the prediction of the diffusion rate of elements (such as C and N) during heat treatment cannot be accurately performed.

This work aims to study the species diffusion and chemical reaction at component surfaces in a fluidised bed heat treatment furnace. The hydrodynamics of the gas fluidised bed is modelled with the Eulerian method. The chemical reaction rates in the bed are calculated by using both the finite rate model (FRM) and the eddy dissipation model (EDM). A mechanism model is used for modelling the reaction and element transfer rates at the component surface.
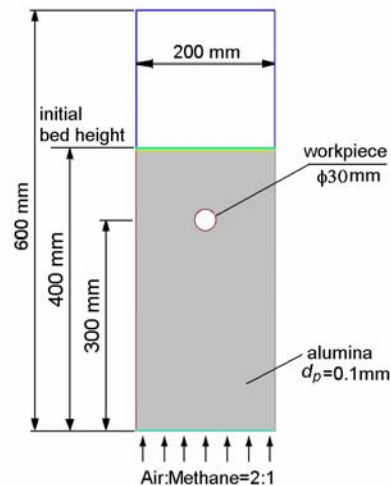
PROBLEM DESCRIPTION

Figure 1. Reaction of methane with air in a gas-solid fluidised reactor
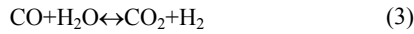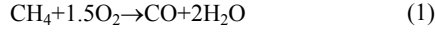
In the current work, the carburisation of a low-carbon steel component with a methane-air mixture in an alumina fluidised bed was simulated. A two-dimensional computational domain is used in the simulation. The fluidised bed is 200 mm in width and 600 mm in height, with 400 mm of the bed filled with alumina particles of 0.1 mm in diameter (d_p) (**Figure 1**). The density of the particles was 3890 kg/m^3. The initial volume fraction of the particles in the bed was 0.54. The steel component was a cylinder with a diameter of 30 mm. To ignite the

reactions, the temperature of the reactor wall was set to be 1300K, thus the reactions started in the region close to the corner between the wall and the bottom. The carburising gas was composed of 1/3 methane and 2/3 air by volume. The initial mixture flowed into the reactor from the bottom with a velocity of 0.06 m/s.

MATHEMATICAL MODELS

Volumetric Reaction Model

The reactions in the bed are expressed by equations (1) (2) and (3). Thus there are seven gases (CH_4, CO, O_2, CO_2, H_2O, H_2 and N_2) in the fluid phase.

$$CH_4 + 1.5O_2 \rightarrow CO + 2H_2O \qquad (1)$$

$$CO + 0.5O_2 \leftrightarrow CO_2 \qquad (2)$$

$$CO + H_2O \leftrightarrow CO_2 + H_2 \qquad (3)$$

Generally, the reactions of fluidising gases are fast. Consequently, the overall rate of the reactions is controlled by turbulent mixing. The turbulence slowly convects and mixes cold reactants and hot products into reaction zones, where reactions occur rapidly. The eddy dissipation model (EDM) is often used for the turbulence-controlled reactions. The reactions proceed whenever turbulence is present ($k/\varepsilon > 0$, where k is turbulent kinetic energy and ε is eddy dissipation rate), and an activation temperature is not required to initiate the reactions. The fluidising gases will react as soon as they enter the reactor. However, generally, the fluidising gases are mixed before flowing into the reactor. Further, there are high-density solid particles in the reactor. The reactions are started by the high-temperature bed wall and the hot solid particles. Therefore, the chemical kinetic rates are also accounted for in the simulation. Since it is not known if the turbulence controls the overall reaction rate or the chemical kinetics, both the finite rate model (FRM) and the eddy dissipation model (EDM) are employed in the present work. That is, both the Arrhenius and eddy dissipation reaction rates are calculated. The slowest rate is the limiting rate of reaction and is used for the calculations,

$$R_{i,r} = \min(R_{i,r}^{Edd1}, R_{i,r}^{Edd2}, R_{i,r}^{Kin}) \qquad (4)$$

The EDM describes the effect of turbulence on the reaction rate. Based on the work of Magnussen and Hjertager (Magnussen and Hjertager, 1976), the net rate of production of species i due to reaction r, $R_{i,r}$, is given by the smaller (i.e., limiting value) of the two expressions below:

$$R_{i,r}^{Edd1} = \nu_{i,r} M_i A \rho \frac{\varepsilon}{k} \min_R \left(\frac{Y_R}{\nu_{R,r} M_R} \right) \qquad (5)$$

$$R_{i,r}^{Edd2} = \nu_{i,r} M_i A B \rho \frac{\varepsilon}{k} \frac{\sum_P Y_P}{\sum_j^N \nu_{j,r} M_j} \qquad (6)$$

where $\nu_{i,r}$ present the stoichiometric coefficient for product i in reaction r. A and B are empirical constants, with values of 4.0 and 0.5, respectively. Y_R and Y_p denote the mass fractions of reactants and products, respectively. M_i M_j and M_R are the molecular weights of species i, species j and reactant R, respectively.

The FRM describes the effect of temperature and concentration of the species on the reaction rate. The rate of reaction for any reactant is assumed to be given by the Arrhenius expression.

$$R_{i,r}^{Kin} = M_i B_r T^{\beta_r} e^{-E_r/RT} \prod_{j=1}^{N_r} \left(\frac{\rho Y_{j,r}}{M_j} \right)^{\nu_{j,r}} \qquad (7)$$

where B_r denotes a pre-exponential factor, E_r is the activation energy of reaction r, R is the universal gas constant, and N_r is the number of chemical species in reaction r.

Chemical Reaction Model at the Steel Surface

The process of carbon transfer from the gas phase to the steel has been well described (Collin, Gunnarson and Thulin, 1972a, Dragomir and Druga, 2001, Gao, et al., 2004). In this work, the carbon transfer at the steel surface is modelled by the following three independent reactions;

$$CH_4 \leftrightarrow [C] + 2H_2 \qquad (8)$$

$$2CO \leftrightarrow [C] + CO_2 \qquad (9)$$

$$CO + H_2 \leftrightarrow [C] + H_2O \qquad (10)$$

where [C] denotes a diffused atom of carbon.

For these the total mass-flow density J, g/cm^2 s, can be calculated by the equation

$$J = \rho \left[\frac{k_1}{a_s}(a_{g1} - a_s) + \frac{k_2}{a_s}(a_{g2} - a_s) + k_3(a_{g3} - a_s) \right] \qquad (11)$$

where, the subscripts 1, 2 and 3 stand for the reactions (8), (9) and (10), respectively. a_s is the carbon activity in the steel.

The reaction-rate coefficients, k, in equation (11) can be described with relationships of the following general form:

$$k = k(T, \text{gas-composition}) \qquad (12)$$

The carbon activity in the gas, a_g, for equations (8)-(10) can be calculated by

$$a_{g1} = K_1 \frac{pCH_4}{pH_2^2} \qquad (13)$$

$$a_{g2} = K_2 \frac{pCO^2}{pCO_2} \qquad (14)$$

$$a_{g3} = K_3 \frac{pCO \cdot pH_2}{pH_2O} \qquad (15)$$

The carbon activities need not be equal for the different reactions. Equation (11), therefore, is valid also when the components of the furnace atmosphere are not in equilibrium.

The equilibrium coefficients K_1, K_2 and K_3 are a function of temperature. Equations for K_1, K_2 and K_3 and the reaction-rate coefficients, k_1, k_2 and k_3, proposed by Collin (Collin, 1976) are used in the present modelling.

Eulerian Multiphase Flow Model

Over the past decades, the hydrodynamics of gas-fluidised beds has been extensively simulated (Feng, Hu and Joseph, 1994, van Wachem, et al., 2001a, Gao, Kong and Hodgson, 2002, Goldschmidt, Beetstra and Kuipers, 2004). The models for fluidised beds can be classified into two main categories based on the modelling method of the solid particles, Eulerian and Lagrangian methods. In the Eulerian method, the individual phases are treated as pseudo-continuous fluids, each being governed by conservation laws expressed in terms of volume per time or ensemble-averaged properties (Anderson and Jackson, 1967, Schmidt and Renz, 2000). The flow fields at sub-particle level are not resolved, and empirical equations are applied for fluid-particle drag. Owing to the continuum description of the particulate suspension, Eulerian models require addition closure laws to described particle-particle and/or particle-wall interactions (Goldschmidt, et al., 2004). In most recent continuum models (Goldschmidt, et al., 2004, Sun and Battaglia, 2006), the kinetic theory of granular flow has been used to build the constitutive equations. This theory is basically an extension of the classical kinetic theory of gases to density particulate flows that takes non-ideal particle-particle collisions and gas-particle drag into account. In the Lagrangian approach, the discrete particles are treated as a group of "point" masses with their position, velocity and other quantities being tracked based on the motion equation of individual particles (van Wachem, van der Schaaf, Schouten, Krishna and van den Bleek, 2001b). An alternative approach to modelling of solid particles is the discrete element method (DEM). The discrete particle models do not require additional closure equations for the suspended particulate phase since they compute the motion of every individual particle, taking collisions and external forces acting on the particles directly into account (Tsuji, et al., 1993, Rhodes, Wang, Nguyen, Stewart and Liffman, 2001b).

The DEM is a simple numerical model by which interactions due to multi-body collisions can be calculated. The particles are traced individually by direct solution of Newton's equation of motion, which enables understanding of the particle motion abd heat and mass transfer processes at the particle level. However, the number of particles that the DEM can handle (typically less than 106) is orders of magnitude lower then that encountered in most fluidised beds. Therefore, continuum models constitute a more natural choice for hydrodynamic modelling of an engineering scale system. To model the fluidisation in large industrial-scale fluidised bed heat

treatment furnaces, the Eulerian method is better than the Lagrangian method due to the computational expense to simulate a large number of particles.

In the Eulerian model, the gas phase and the suspended particulate phase are considered to be continuum and fully interpenetrating. The governing equations for fluid phase (*f*) and solid phase (*s*) are given by

Continuity equations

$$\frac{\partial(\varepsilon_f \rho_f)}{\partial t} + \nabla \bullet (\varepsilon_f \rho_f \vec{\upsilon}_f) = \dot{m}_{sf} - \dot{m}_{fs} \qquad (16)$$

$$\frac{\partial(\varepsilon_s \rho_s)}{\partial t} + \nabla \bullet (\varepsilon_s \rho_s \vec{\upsilon}_s) = \dot{m}_{fs} - \dot{m}_{sf} \qquad (17)$$

Momentum equations

$$\frac{\partial(\varepsilon_f \rho_f \vec{\upsilon}_f)}{\partial t} + \nabla \bullet (\varepsilon_f \rho_f \vec{\upsilon}_f \vec{\upsilon}_f) = -\varepsilon_f \nabla p \\ + \varepsilon_f \rho_f \vec{g} + \nabla \bullet \overline{\overline{\tau}}_f - \beta(\vec{\upsilon}_f - \vec{\upsilon}_s) \qquad (18)$$

$$\frac{\partial(\varepsilon_s \rho_s \vec{\upsilon}_s)}{\partial t} + \nabla \bullet (\varepsilon_s \rho_s \vec{\upsilon}_s \vec{\upsilon}_s) = -\varepsilon_s \nabla p \\ - \nabla p_s + \varepsilon_s \rho_s \vec{g} + \nabla \bullet \overline{\overline{\tau}}_s + \beta(\vec{\upsilon}_f - \vec{\upsilon}_s) \qquad (19)$$

where ε is volume fraction; υ is velocity; ρ is density; p is pressure; $\overline{\overline{\tau}}$ is stress tensor; g is the gravity constant (9.816 m/s^2); and m characterises the mass exchange between phases.

The interaction between gas and solid particles in gas-solid systems has been well understood (Fan and Zhu, 1998, van Wachem, et al., 2001a, Gao, et al., 2002, Goldschmidt, et al., 2004). In the dense regime (ε_f <0.8), the momentum transfer coefficient, β, can be obtained from the well-known Ergun equation,

$$\beta = 150 \frac{(1-\varepsilon_f)^2 \mu}{\varepsilon_f^3 d_p^2} + 1.75 \frac{(1-\varepsilon_f)\mu \operatorname{Re}_p}{\varepsilon_f^3 d_p^2} \qquad (20)$$

where μ is the viscosity of the fluid phase.

For the dilute regimes (ε_f ≥0.8), the coefficient can be derived from the correlation of Wen and Yu (Wen and Yu, 1966),

$$\beta = \frac{3}{4} \frac{(1-\varepsilon_f)\mu C_D \operatorname{Re}_p}{\varepsilon_f^{2.65} d_p^2} \qquad (21)$$

Where the drag coefficient, C_D, is given by

$$C_D = \begin{cases} \dfrac{24}{\text{Re}_p}(1+0.15\text{Re}_p^{0.687}) & \text{Re}_p < 1000 \\[2mm] 0.44 & \text{Re}_p \geq 1000 \end{cases} \qquad (22)$$

The Reynolds number is calculated by

$\text{Re}_p = \rho d_p \left| \upsilon_f - \upsilon_s \right| / \mu$.

The solid phase pressure, p_s, that prevents particles from reaching impossibly low values of void fraction was modelled as

$$p_s = \varepsilon_s \rho_s \Theta_s + 2\rho_s(1+e_{ss})\varepsilon_s^2 g_{0,ss}\Theta_s \qquad (23)$$

In the Eulerian model, the actual particle velocity is decomposed into a local mean velocity (υ_s) and a random fluctuation velocity (C_s). The kinetic energy of the random motion of the particles is described with the so-called granular temperature,

$$\Theta_s = \frac{1}{3} \left\langle \overline{C_s} \bullet \overline{C_s} \right\rangle \qquad (24)$$

where $\langle\ \rangle$ is the ensemble average.

The granular temperature conservation equation is

$$\frac{3}{2}\frac{\partial(\varepsilon_s\rho_s\Theta_s)}{\partial t} + \nabla \bullet (\varepsilon_s\rho_s\vec{\upsilon}_s\Theta_s) = \\ (-p_s\overline{\overline{I}} + \overline{\overline{\tau}}_s):\nabla\vec{\upsilon}_s + \nabla\bullet(k_{\Theta s}\nabla\Theta_s) - \gamma\Theta_s - 3\beta\Theta_s \qquad (25)$$

In the present simulation, the constitutive equations for the solid stress tensor ($\overline{\overline{\tau}}_s$) and the diffusive flux of granular energy ($k_{\Theta s}$) are calculated with the Syamlal et al. model (Fluent-Incorporation, 2005). The collisional dissipation of energy ($\gamma\Theta_s$) is represented by the expression derived by Lun et al. (Lun, Savage, Jeffrey and Chepurniy., 1984).

To describe the effect of turbulent fluctuations of velocities, the standard k-ε turbulence model is applied for each phase.

Energy and Species Diffusion Equations

Enthalpy equations were used to describe the energy conservation for each phase. The enthalpy change due to a chemical reaction is taken into account in the enthalpy conservation of the gas phase,

$$\frac{\partial(\varepsilon_p\rho_p h_p)}{\partial t} + \nabla\bullet(\varepsilon_p\rho_p\vec{\upsilon}_p h_p) = -\varepsilon_p\frac{\partial p_p}{\partial t} \\ + \overline{\overline{\tau}}_p:\nabla\vec{\upsilon}_p - \nabla\bullet\vec{q}_p + Q_p + \sum_r \eta_{gr}(-\Delta H_r)R_r \qquad (26)$$

where $p=f$ for fluid phase or s for solid phase, h is the specific enthalpy, $\vec{q}$ is the heat flux, Q is the heat exchange between phases, and $\eta_{g,r}$, ΔH and R_r are the distribution ratio of reaction heat of gas g, the enthalpy change and the reaction rate for reaction r, respectively.

In particular, the process includes the transport of gaseous molecules from the heat treatment atmosphere to the steel surface through the boundary layer, the decomposition of gaseous molecules at the gaseous atmosphere/steel surface interface, the absorption of atoms in the steel surface and carbon dissolution. The process is further complicated by the presence of solid particles in the system.

In a heat treatment furnace, the atmosphere is composed of several chemical species. The local mass fraction of each species, Y_i, is predicted through the solution of a convection-diffusion equation for the ith species.

$$\frac{\partial(\varepsilon_f\rho_f Y_i)}{\partial t} + \nabla\bullet(\varepsilon_f\rho_f\vec{\upsilon}_f Y_i) = \\ \nabla\bullet(\varepsilon_f\rho_f D_i\nabla Y_i) + \sum_r \nu_{i,r}R_{i,r} \qquad (27)$$

SOLUTION

In this work, a commercial software package, FLUENT, was used to implement the simulation. The componential domain was meshed with quadrilateral elements. The size of elements was 2 mm, except the elements in the region around the cylinder workpiece. The boundary on the workpiece surface was refined into 10 layers, as shown in **Figure 2**. The height of the row nearest to the workpiece surface was 0.2 mm. The growth factor, that is the ratio of the height of each row relative to that of the immediately preceding row, was 1.2.
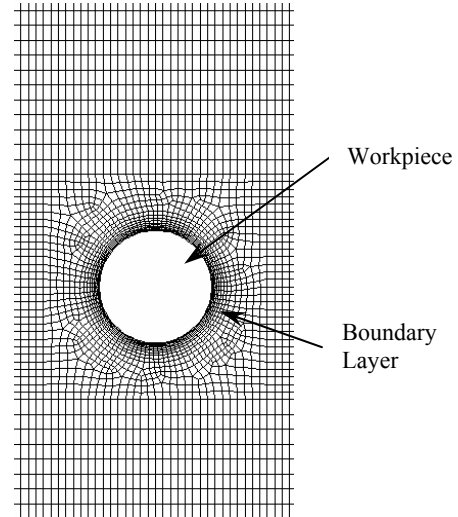

Figure 2. Refinement of mesh for the region around workpiece

The governing equations were solved sequentially. Because the equations are non-linear and coupled, several iterations of the solution loop were performed before a convergence was achieved. The continuous phase flow field and temperature were initialized with resting air with a given temperature (300 K). The momentum and energy

equations were firstly solved to update the velocity and temperature fields. Chemical reaction rates and species diffusion were calculated using the previously calculated temperature and turbulent diffusion rate.

RESULTS

Figure 3 shows the carbon transfer coefficient around the component and the contribution of each surface reaction. It can be seen that the total carbon transfer coefficient at the lift side of the component (from 138°-207°) is much lower than that at other mass transfer positions. The average carbon transfer coefficient on the component surface of 138°-207° is 1.25×10^{-5} cm/s, which is in good agreement of the experimental results of Gao (Gao, 2004), who measured the carbon transfer coefficient around a workpiece immersed in an industrial fluidized bed heat treatment furnace. Gao et al (Gao, et al., 2004) also proposed an empirical equation to predict the carbon transfer coefficient at the vertical surface of the workpiece. For the same carburizing conditions as used in the simulation, the carbon transfer coefficient predicted with the empirical equation is 1.38×10^{-5} cm/s.
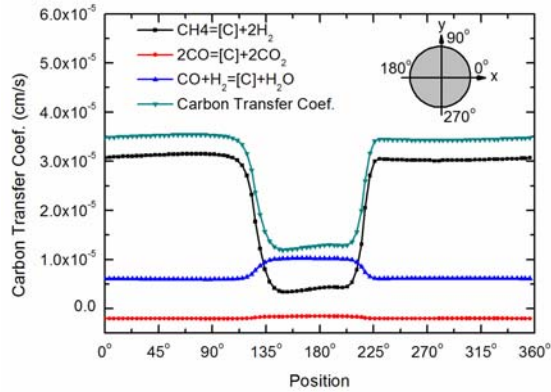

Figure 3. The carbon transfer coefficient at component surface and the contribution of each carburizing reaction

At the component surface of 138°-207°, the carbon transfer coefficient is dominated by the reaction of (10). The methane and CO reactions (8) and (9) are very slow in comparison with reaction (10). This is often observed in production furnaces. The same results and the contribution of different carburizing reactions were also reported by Collin (Collin, Gunnarson and Thulin, 1972b) for the carburizing atmosphere of 0.6% CH_4, 31.5% H_2, 23.5% CO, 0.17% CO_2 and 0.33% H_2. This is because the water-gas reaction (3) is assumed to go to equilibrium. A change in CO_2 concentration will influence the H_2O concentration and also the reaction (10).

High carbon transfer coefficient is found at the right side of the component (230°-360°-110°). **Figure 3** also shows that the carbon transfer at this region is mainly attributed to reaction (8), due to the high concentration of CH_4.

The carbon transfer coefficient is a function of the temperature and the composition of the gas close to the component. The simulation shows that the temperatures at different component surfaces are the same, because of the high conductivity of steel and the small size of the component used in the present work. **Figure 4** shows the gas composition and the distribution of mole fraction for

each species. It can be stated that the carbon transfer coefficient at the component surface is corresponding to the gas composition. Higher mole fraction of carbonizing reactants (CO and H_2) can be found in the region close to the left side of the component, while the concentration of CH_4 in the region of 230°-110° is much higher than that in the other positions (**Figure 4**). The high CH_4 concentration is due to the low reaction rate of methane and air. This is seldom found in production heat treatment fluidised beds operated at an optimized operation condition. The large difference in the species concentration is a result of the hydrodynamic simulation of the gas-fluidised bed.
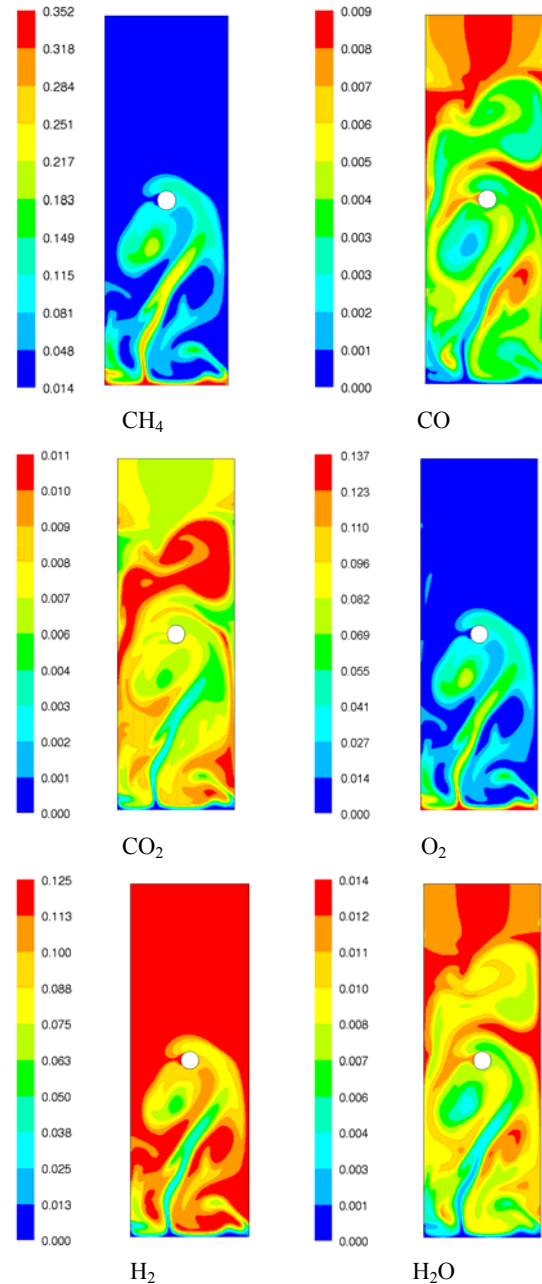

Figure 4. Distribution of mole fraction for different gases (%) (t=2.6 s)

Figure 5 shows the volume fraction of the solid particles in the bed at different times. It can be seen that a tube was

5

formed in the central lower section of the bed, where the particulate volume fraction is very low (about 0.25). This leads to high gas velocity and low temperature. As a result, the reaction rate of CH_4 and O_2 will be reduced. As shown in **Figure 4**, high CH_4 and O_2 concentrations were found in this region.
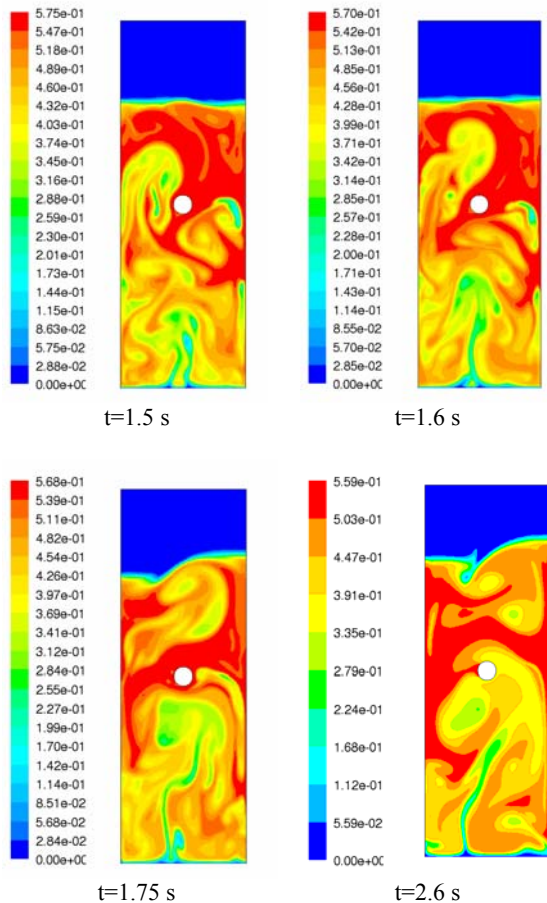

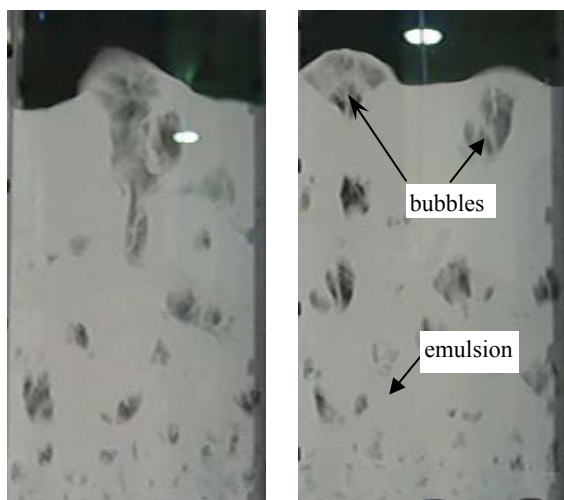**Figure 5.** Distribution of volume fraction of solid particles

Figure 6. Solid particle concentration in an experimental fluidised bed

For the particles used in the present simulation, good bubbling fluidisation should be achieved in the bed (Kunii and Levenspiel, 1991). A bubbling fluidised bed has some low solid density regions called bubbles and a higher solid density region called the emulsion, as shown in Figure 6. Comparing the simulation results (Figure 5) with the experimental results (Figure 6) shows that the improvement of hydrodynamic simulation is required.

CONCLUSION

An integrated model was developed to simulate the mass transfer and species diffusion at a steel component surface in a heat treatment fluidised bed. A standard k-ε turbulent model, an Eulerian multiphase flow model, a chemical reaction kinetic model, an eddy dissipation model and a solid-surface chemical reaction model were used for the simulation.

Using the developed model, a carburising process of a steel component in a fluidised bed of 0.1 mm alumina particles was simulated. The simulation results show that the chemical reaction models can correctly predict the mass transfer rate at the steel surface. A good agreement between the predicted and measured carbon transfer coefficients was found at some component surfaces. However, the carbon transfer at other surfaces was over-predicted, due to the hydrodynamic simulation. The disparity seen between the simulated distribution of solid particles and the solid particle concentration in an experimental fluid bed indicated a refinement of the hydrodynamic model is required.

REFERENCES

ANDERSON, T. B., and JACKSON, R. (1967), "A fluid mechanical description of fluidized beds," *I&EC Fundam.*, 6, 527.

COLLIN, R. (1976), "Mass-transfer characteristics of carburizing atmospheres," in *Heat treatment '76: Pro. of the 16th Int. Heat Treatment Conf.*, Stratford-upon-Avon, pp. 121-124.

COLLIN, R., GUNNARSON, S., and THULIN, D. (1972a), "Influence of reaction rate on gas carburizing of steel," *J. of the Iron and Steel Institute*, 777-784.

COLLIN, R., GUNNARSON, S., and THULIN, D. (1972b), "A mathematical model for predicting carbon concentration profiles of gas-carburized steel," *J. of the Iron and Steel Institute*, 785-789.

DRAGOMIR, D., and DRUGA, L. (2001), "The advantages of fluidized bed carburizing," *Materials Science & Engineering, A: Structural Materials: Properties, Microstructure and Processing*, 302, 115-119.

FAN, L. S., and ZHU, C. (1998), *Principles of gas-solid flows*, Cambridge, U.K.: Cambridge University Press.

FENG, J., HU, H. H., and JOSEPH, D. D. (1994), "Direct simulation of initial value problems for the motion of solid bodies in a Newtonian fluid. Part 1. Sedimentation," *J.l of Fluid Mechanics*, 261, 95-134.

FLUENT-INCORPORATION. (2005), "Fluent 5.2.16."

GAO, W. M. (2004), "*Heat and mass transfer in fluidised-bed heat-treatment furnaces*," PhD Thesis,

Deakin University, School of Engineering and Technology.

GAO, W. M., HODGSON, P. D., and KONG, L. X. (2005), "Experimental investigation and numerical simulation of heat transfer in quenching fluidised beds," *Int. J. Materials & Product Technology*, 24, 325-344.

GAO, W. M., KONG, L. X., and HODGSON, P. D. (2002), "Numerical simulation of heat and mass transfer in fluidised bed heat treatment furnaces," *J. of Materials Processing Technology*, 125-126, 170-178.

GAO, W. M., LONG, M. J., KONG, L. X., and HODGSON, P. D. (2004), "Influence of the geometry of an immersed steel workpiece on mass transfer coefficient in a fluidised bed furnace," *ISIJ International*, 44, 869-877.

GOLDSCHMIDT, M. J. V., BEETSTRA, R., and KUIPERS, J. A. M. (2004), "Hydrodynamic modelling of dense gas-fluidised beds: comparison and validation of 3D discrete particle and continuum models," *Powder Technology*, 142, 23-47.

KUNII, D., and LEVENSPIEL, O. (1991), *Fluidization engineering*, Krieger, Huntington, New York: Butterworth-Heinemann.

LUN, C. K. K., SAVAGE, S. B., JEFFREY, D. J., and CHEPURNIY, N. (1984), " Kinetic theories for granular flow: Inelastic particles in Couette flow and slightly inelastic particles in a general flow field.," *J. of Fluid Mechanics*, 140, 223-256.

MAGNUSSEN, B. F., and HJERTAGER, B. H. (1976), "On mathematical models of turbulent combustion with special emphasis on soot formation and combustion," in *16th Symp. (Int.) on Combustion*, Cambridge, MA: The Combustion Institute, p. 719.

RHODES, M. J., WANG, X. S., NGUYEN, M., STEWART, P., and LIFFMAN, K. (2001a), "Onset of cohesive behaviour in gas fluidized beds: A numerical study using DEM simulation," *Chemical Engineering Science*, 56, 4433-4438.

RHODES, M. J., WANG, X. S., NGUYEN, M., STEWART, P., and LIFFMAN, K. (2001b), "Study of mixing in gas-fluidized beds using a DEM model," *Chemical Engineering Science*, 56, 2859-2866.

SCHMIDT, A., and RENZ, U. (2000), "Numerical prediction of heat transfer in fluidized beds by a kinetic theory of granular flows," *Int. J. of Thermal Sciences*, 39, 871-885.

SUN, J., and BATTAGLIA, F. (2006), "Hydrodynamic modeling of particle rotation for segregation in bubbling gas-fluidized beds," *Chemical Engineering Science*, 61, 1470-1479.

TSUJI, Y., KAWAGUCHI, T., and TANAKA, T. (1993), "Discrete particle simulation of a fluidized bed," *Powder Technology*, 77, 79.

van WACHEM, B. G. M., SCHOUTEN, J. C., van den BLEEK, C. M., KRISHNA, R., and SINCLAIR, J. L. (2001a), "Comparative analysis of CFD models of dense gas-solid systems," *AIChE J.*, 47, 1035-1051.

van WACHEM, B. G. M., van der SCHAAF, J., SCHOUTEN, J. C., KRISHNA, R., and van den BLEEK, C. M. (2001b), "Experimental validation of Lagrangian-Eulerian simulations of fluidized beds," *Powder Technology*, 116, 155-165.

WEN, C. Y., and YU, Y. H. (1966), "Mechanics of fluidization," *Chem. Engng. Prog. Symp. Ser.*, 62, 100-108.

ZHENG, Y., WAN, X., QIAN, Z., WEI, F., and JIN, Y. (2001), "Numerical simulation of the gas-particle turbulent flow in riser reactor based on k-ε-k_p-ε_p-T two-fluid model," *Chem. Eng. Sci*, 56, 6813-6822.